

# On the robustness of reduced-order jet noise models

Vasily Gryazev,<sup>1</sup>

*Queen Mary University of London, Mile End Road, London, E1 4NS, United Kingdom*

Annabel P. Markesteijn<sup>2,4</sup>, and Sergey A. Karabasov<sup>3,4</sup>

*Queen Mary University of London, Mile End Road, London, E1 4NS, United Kingdom  
GPU-prime Ltd, 16 St. Thomas Close, Comberton, Cambridge, CB23 7DN, United Kingdom*

**Three statistical jet noise prediction models are compared for a representative set of single-stream jet cases, which include cold and hot jets of the Strategic Investment in Low-carbon Engine Technology (SILOET) experiment at acoustic Mach number 0.875 and the cold jets of the NASA Small Hot Jet Acoustic Rig (SHJAR) experiment at acoustic Mach numbers 0.5 and 0.9. The implemented models are those proposed by Tam and Auriault, Khavaran, and the Goldstein Generalised Acoustic Analogy (GAA). By the virtue of reduced-order modelling, which is based on the single-point meanflow and turbulence statistics, all these implementations use a number of empirical dimensionless source parameters for far-field noise spectra predictions. In comparison with the Tam and Auriault model, the Khavaran and GAA model implementations use several dimensionless parameters, which are available from the previous literature and assumed to be more-or-less universal for a class of single-stream jets. These parameters include the fluctuating enthalpy function and the dimensionless amplitudes of auto-covariances of turbulent fluctuating stresses and velocities available from the literature. The comparison of the three models is aimed not only at assessing their accuracy for a range of jet conditions, observer angles, and frequencies, but also to examine their robustness outside of a reference jet experiment for which their source models were calibrated. For the input to each model, the meanflow, turbulence kinetic energy, and dissipation rate extracted from Large Eddy Simulations**

---

<sup>1</sup> Post-Doctoral Researcher, School of Engineering and Material Sciences and AIAA member

<sup>2</sup> Post-Doctoral Researcher, School of Engineering and Material Sciences and AIAA member

<sup>3</sup> Professor, School of Engineering and Material Sciences and AIAA Associate Fellow

<sup>4</sup> Research Scientist / Director, GPU-prime Ltd

The preliminary version of the manuscript was presented at AIAA Conference: Gryazev, V., Karabasov, S.A., “Comparison of two Goldstein acoustic analogy implementations with the Tam&Auriault model for heated and unheated jet noise prediction”, AIAA Aeroacoustics Conference, 25-29 June, Atlanta, 2018.

**(LES) and Reynolds-Averaged Navier-Stokes (RANS) solutions are considered. Insights and perspectives of using these models in future multidisciplinary design optimisation studies are discussed.**

### **Nomenclature**

|                |   |  |
|----------------|---|--|
| $c$            | = | Speed of sound                                     |
| $\frac{D}{Dt}$ | = | Convective derivative                              |
| $\alpha$       | = | Non-dimensional momentum source amplitudes         |
| $\beta$        | = | Non-dimensional enthalpy source amplitudes         |
| $c_l$          | = | Turbulent length scale empirical constant          |
| $c_\tau$       | = | Turbulent time scale empirical constant            |
| $D_j$          | = | Jet diameter                                       |
| $\delta_{ij}$  | = | Kronecker symbol                                   |
| $p$            | = | Pressure   |
| $\rho$         | = | Density  |
| $v_1$          | = | Axial velocity component                           |
| $U$            | = | Mean velocity                                      |
| $\mathbf{x}$   | = | Position vector of the observer                    |
| $\mathbf{y}$   | = | Position vector of the source                      |
| $T$            | = | Temperature  |
| $t$            | = | Time   |
| $r$            | = | Radial coordinate                                  |
| $y_1$          | = | Axial coordinate                                   |
| $\theta$       | = | Azimuthal angle in the jet coordinate frame system |

- $\varphi$  = Observer angle to the jet axis  
 $\kappa$  = Turbulent kinetic energy  
 $h$  = Enthalpy  
 $n$  = Mode number  
 $\tau$  = Time delay ( $\tau = t_1 - t_2$ )  
 $\omega$  = Angular frequency ( $2\pi f$ )  
 $\mathcal{E}$  = Turbulent dissipation rate  
 $\xi$  = Meanflow vorticity  
 $M$  = Mach number ( $U_j / c_\infty$ )  
 $M_c$  = Convective Mach number ( $U_c / c_\infty$ )  
 $l_s$  = Turbulence length scale  
 $\tau_s$  = Turbulence time scale  
 $St$  = Strouhal number  
 $S_T$  = Power Spectral Density estimated by Tam and Auriault's model  
 $S_K$  = Power Spectral Density estimated by Khavaran's model  
 $S_G$  = Power Spectral Density estimated by Generalised acoustic analogy model  
 $k$  = Wave number magnitude ( $\omega / c_\infty$ )  
 $R$  = The far-field arc distance from jet exit,  
 $\langle \cdot \rangle$  = Averaging over defined interval

### *Subscripts*

- $i, j, k, l$  = Vector or tensor components  
 $C$  = Related to cold jet  
 $H$  = Related to hot jet

- $D$  = Based on jet diameter
- $\infty$  = Ambient condition
- $c$  = Convection variable
- $j$  = Jet exit condition
- $t$  = Total
- $s$  = Source related variable

*Superscripts*

- $(a)$  = adjoint variable
- $\bar{\cdot}$  = Time averaged
- $\tilde{\cdot}$  = Favre averaged
- $\cdot'$  = Fluctuating component
- $\hat{\cdot}$  = Fourier transform

## I. Introduction

Mitigation of noise of high-speed propulsive jets remains of importance for aircraft at take-off conditions, which has received renewed attention due to the recent interest in commercial supersonic flight [1]. In the past, an effective method to reduce jet noise has been to increase the bypass ratio of jet engines, which reduces the exhaust flow velocity, thereby diminishing the acoustic power that scales with a high power of the jet velocity. However, the increase of bypass ratio as a method of jet noise reduction has limitations because it comes with the engine size increase, hence, a reduction of distance between the jet nozzle and the airframe leads to additional jet installation noise [2,3]. A number of jet noise reduction technologies were proposed, such as chevron and non-concentric dual-stream nozzles, which modify the jet flow and turbulence by changing the nozzle geometry [4-9]. The design of such non-axisymmetric nozzles is a challenging multidisciplinary problem, where the improved aeroacoustic performance must not compromise the thrust.

While the aeroacoustic-aerodynamic optimisation using high-fidelity methods such as Large Eddy Simulation (LES) still remains expensive [10], previous works in the area of acoustic optimization [11,12] used reduced-order

models based on the Reynolds-Averaged Navier–Stokes (RANS) flow solutions in a design optimization loop with noise prediction schemes of acoustic analogy-type. The steady-state RANS models have been traditionally used by industry in the aerodynamic design because they are not expensive compared to the high-fidelity models such as those based on Large Eddy Simulations, while allowing one to capture a change in the jet aerodynamics due to a change in the nozzle geometry. For the use in aeroacoustic optimisation, however, the statistical quantities available from the RANS flow solution must be combined with a suitable model of the effective acoustic source, which step involves significant assumptions.

In many RANS-based acoustic models, the source amplitude is scaled on the turbulent kinetic energy squared, and the corresponding space and time scales of the source are reconstructed from the turbulence kinetic energy and the turbulence dissipation rate using empirical proportionality coefficients [13-18]. Alternatively, following [19], similar proportionality coefficients for the acoustic space and time length scale modelling can be obtained from the turbulence kinetic energy and the meanflow vorticity. The proportionality coefficients are usually adjusted for the baseline jet conditions and are assumed to be constant during the design optimization cycle. While this assumption allows to significantly simplify the modelling, its validity may vary from case to case depending on the sensitivity of the acoustic analogy model used to the empirical coefficients, and how far the optimal design geometry is from the baseline conditions. At the same time, to the best of the authors' knowledge, there has been no investigation, which would systematically analyse the sensitivity of RANS/LES-based jet noise models to the source model parameters for jet flows at a high Reynolds number of industrial relevance. The goal of this work is to partly fill this gap for three well-established jet noise models. Having fixed the source model parameters and compared the models' performance for one jet condition (experiment), we will analyse the sensitivity of the predictions of the same models to a variation of the jet experiment. To quantify uncertainties related to the turbulence modelling, the acoustic modelling will be based on the same time-averaged flow quantities extracted from a RANS solution and a Large Eddy Simulation (LES) in each case.

The first model to consider is the fine-scale jet mixing noise model of Tam and Auriault [13, 20], which is one of the most popular in jet noise literature. In this model, the effective acoustic source is represented by an auto-covariance of the convective derivative of fluctuating Reynolds stresses. The auto-covariance function is approximated by a Gaussian-exponential shape function, which is integrated analytically. The sources are grouped in one isotropic term inspired by analogy with the kinetic gas theory without distinguishing between either the cold

and hot jet noise sources or individual source terms of different directivity. As it was pointed out by Morris and Farassat [22], the Tam and Auriault model can also be obtained from the Lighthill acoustic analogy formalism [21].

The second considered jet noise model corresponds to the model of Khavaran and co-workers [17, 23-25], which is used in NASA's JeNo code. Similar to the Tam model, the Khavaran model considers the sound sources in the reference frame moving with the jet flow and combines the contributions of individual fluctuating Reynolds stresses in a single term. However, in comparison with the Tam and Auriault model, a separate fluctuating enthalpy source model is included in the Khavaran model for hot jet noise predictions [25]. The fluctuating enthalpy model is based on empirical parameters such as a function to approximate the enthalpy fluctuations via the temperature gradient and Nozzle Pressure Ratio (NPR). In addition, an empirical convection speed function is used, which depends on both the jet local velocity and the velocity at the nozzle exit.

The third jet noise model corresponds to the Goldstein Generalised Acoustic Analogy (GAA) [26, 27]. Specifically, out of many possible implementations of GAA, the one considered in this work corresponds to [19, 28]. Following the Khavaran model, the implemented GAA model uses a separate source term for hot jet noise modelling. The sources of the GAA model are considered in the stationary nozzle frame, thereby using the covariance of fluctuating turbulence stresses and the velocity auto-correlation function with no material derivative involved. Due to the absence of the derivative operator, the acoustic source terms of GAA become amenable for modelling term-by-term using the LES data from which the turbulent fluctuating stresses are readily available. In this work, the relative amplitudes of the individual source terms obtained from the previous LES calculation are used [19]. In comparison with the Tam and the Khavaran models, the GAA model retains the individual directivity of several major source terms for the cold and the hot noise source components.

The SILOET (Strategic Investment in Low-carbon Engine Technology) data provide the common anchoring point for the three jet noise models. The two jets considered are issued from a profiled convergent nozzle at the same acoustic Mach number 0.875 in the experiment performed by QinetiQ. The accuracy of the models is examined based on the input such as the choice of the flow solutions (RANS, LES) as well as the assumptions used to define the acoustic correlation scales (based on the turbulent kinetic energy with turbulence dissipation rate or the meanflow vorticity). Then, without any readjustment of the acoustic source parameters, the three acoustic models are applied for far-field noise predictions of the two NASA Small Hot Jet Acoustic Rig (SHJAR) jets corresponding to Set Point (SP) 3 and 7, and their results are compared with the NASA data. In addition, since the Tam and the

Khavaran models were originally calibrated on the NASA jet noise database, the accuracy of one of them (the Tam model) with the source parameters readjusted for the SP7 case is further assessed for noise predictions of the cold SILOET jet experiment.

Preliminary results of this work were presented in [29] and the present article includes extended results and analyses.

The paper is organised as follows. In Section II, the SILOET and the NASA SHJAR jet cases are presented, and the LES and RANS flow solution methodologies are outlined. In Section III, the implemented jet noise models are summarised and their source parameters are defined. Acoustic results are presented in Section IV, which is followed by conclusions in Section V.

## II. Jet Flow Modelling

The first two single-stream static jet flows considered in this work correspond to the SILOET experiment. One of the jets is isothermal and the other is heated, which for brevity will be further referred to as “Cold” and “Hot”. Operating conditions of the SILOET jets are summarised in Table 1.

**Table 1. The operating conditions of SILOET jet.**

| Jet  | $U_j$ | $M_j$ | $T_j / T_\infty$ | Re             |
|------|-------|-------|------------------|----------------|
| Cold | 297   | 0.875 | 1                | $2 \cdot 10^6$ |
| Hot  | 297   | 0.55  | 2.5              | $5 \cdot 10^5$ |

The other two high-speed jets considered in this work correspond to NASA SHJAR Set Point 3 and 7, which details are summarised in Table 2. In comparison with the SILOET jets, both the NASA jets are cold and correspond to different acoustic Mach numbers.

**Table 2. The operating conditions of NASA SHJAR jet.**

| Set Point (SP) | $M_a$ | $T_j / T_0$ | NPR   | $M_j$ |
|----------------|-------|-------------|-------|-------|
| 3              | 0.5   | 0.950       | 2.297 | 0.513 |
| 7              | 0.9   | 0.835       | 2.861 | 0.985 |

For all four jet cases, the LES computations were performed using the Compact Accurately Boundary-Adjusting high-REsolution Technique (CABARET) [30-33]. For turbulence modelling, the Monotonically Integrated LES (MILES) method [34] was used. To speed up the simulations, which use locally refined unstructured OpenFOAM sHM meshes, the method is implemented on Graphics Processing Units (GPU). This strategy allows for generating a useful LES time signal over 400 convective time units on 60-90 million cell grids in a short turnaround time of 2 to 3 days [35-39]. Due to the uniform grid refinement in the early shear layers, a more-or-less isotropic grid of sufficient density is generated near the nozzle lip. For validation in comparison with the far-field acoustic spectra available, the LES flow solutions were combined with the Ffowcs Williams – Hawkings method [40]. Further details of the LES solutions for the SILOET jets are available in [19] and those for the NASA jets are provided in [36].

In addition to the LES, RANS solutions are obtained for the same four jet cases using a density-based solver in ANSYS Fluent with an axi-symmetric body-fitted structured curvilinear grid. The standard free inlet condition is imposed at the nozzle inlet and the corresponding far-field conditions are used at the downstream and lateral boundaries. Following [41], a modification of the  $\kappa$ - $\mathcal{E}$  RANS model parameters is used, which leads to a good agreement of the potential core length in the RANS solution compared to the LES for the four jet cases considered.

Instantaneous snapshots of the velocity and pressure distributions in the jet symmetry plane for the two SILOET and NASA SP3 and SP7 jets are illustrated in Fig.1. The contour levels are adjusted for the best visibility for each top and bottom plot. As expected from the jet physics, the flows considered show a variation of the potential core length depending on the temperature (the potential core is longer in the cold jet compared to the hot) and the jet speed (the potential core is longer in the higher Mach number jet compared to the slower jet). It can also be noted that the pressure waves propagating outside of the jet shear layers form a more distinct wave structure in the case of the noisier jets, i.e. the cold SILOET and the NASA SP7 jets in comparison with the hot SILOET jet and the NASA SP3 jets, respectively. The latter is in agreement with the experimental observations where jet noise increases with the jet velocity and decreases with the jet temperature in subsonic jets [42].

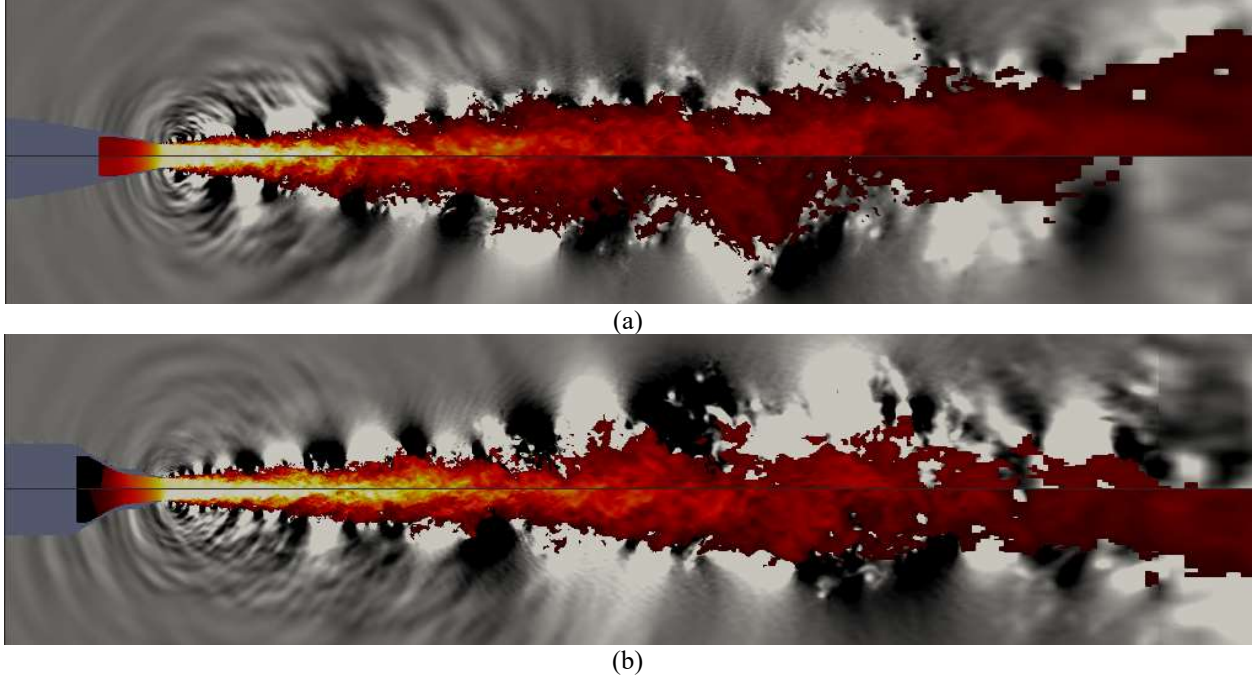


**Fig. 1** Instantaneous velocity and pressure field distributions from the LES solution of the cold (top) and hot (bottom) SILOET jets (a); and NASA SHJAR SP 3 (top) and SP 7 (bottom) jets (b).

### III. Acoustic Models

Key features of the three acoustic source models implemented in the current study, Tam and Auriault's model [13, 43], Khavaran's model [17,25] and the Goldstein Generalised Acoustic Analogy model version of [19] are summarised in Table 3. In all cases, the standard locally parallel flow sound propagation approximation is used, which assumes a slow flow variation in the streamwise direction in comparison with the variation in the radial direction. Further, to simplify the acoustic integration, the radially compact source scale approximation is applied, which neglects the acoustic wavelength variation in the jet shear layer in comparison with the turbulence length scale in the radial direction.

**Table 3. Summary of jet noise source models**

| Features                           | Tam and Auriault | Khavaran | GAA |
|------------------------------------|------------------|----------|-----|
| Momentum source                    | yes              | yes      | yes |
| Enthalpy source                    | no               | yes      | yes |
| Individual source term directivity | no               | no       | yes |

|  |                   |     |     |
|--|-------------------|-----|-----|
| Number of the calibration parameters to be adjusted using the far-field noise data | 3                 | 6   | 2   |
| Applicable observer angles   | close to sideline | all | all |

### A. Tam and Auriault's model

In the fine-scale jet mixing noise model of Tam and Auriault [13], an isotropic noise source is postulated. Hence, by construction, this model is not suitable for noise predictions at peak jet noise angles, where the acoustic field has a highly directional character associated with the large-scale coherent structures [44]. The far-field pressure is expressed as a convolution of the pressure-like component of the vector adjoint Green's function and the convective derivative of an effective source term, which agglomerates momentum terms of the governing linearised Euler equations,

$$p(\mathbf{x}, t) = \int_V \int_{-\infty}^{\infty} \left( \int_{-\infty}^{\infty} p^{(a)}(\mathbf{y}, \mathbf{x}, \omega) \exp(-i\omega\tau) d\omega \right) \frac{Dq_s(\mathbf{y}, t_1)}{Dt_1} dt_1 d\mathbf{y} , \quad (1)$$

where  $q_s \equiv \frac{2}{3} \rho \kappa_s$  is a noise source term in a turbulent flow,  $\kappa_s$  is the kinetic energy of the fine-scale turbulence per unit mass [13], and  $p^{(a)}$  is the adjoint pressure component of the Green's function, which is expanded into Fourier azimuthal harmonics,

$$p^{(a)}(\mathbf{y}, \mathbf{x}, \omega) = \frac{\exp[-ik(R - y_1 \cos \varphi)]}{4\pi R c_\infty^2} \sum_{n=0}^{\infty} f_n \cos n\theta, \quad (2)$$

wherein  $f_n$  are the azimuthal amplitudes satisfying a second-order ordinary-differential equation [43].

By expressing the power spectral density via the frequency-domain pressure amplitude and using the empirical exponential-Gaussian function to model the emerging two-time two-space auto-correlation function in the moving reference frame,

$$\overline{\frac{Dq_s(\mathbf{y}, t_1)}{Dt_1} \frac{Dq_s(\mathbf{y} + \Delta, t_2)}{Dt_2}} \sim \exp \left[ -\frac{|\Delta_1|}{\tilde{v}_1 \tau_s} - \frac{\ln 2}{l_s^2} \left( (\Delta_1 - \tilde{v}_1 \tau)^2 + \Delta_2^2 + \Delta_3^2 \right) \right], \quad (3)$$

where  $\Delta_1, \Delta_2, \Delta_3$  are two-point separation distances in the jet axial, radial, and azimuthal direction, respectively.

After a series of rearrangements involving integrations over  $\tau, \Delta_1, \Delta_2$  and  $\Delta_3$ , the final prediction formula for the far-field noise spectra is obtained,

$$S_T(\mathbf{x}, \omega) = 4\pi \left( \frac{\pi}{\ln 2} \right)^{3/2} \int_V |p^{(a)}(\mathbf{y}, \mathbf{x}, \omega)|^2 \frac{\hat{q}_s^2 l_s^3}{c^2 \tau_s} \frac{\exp[-\omega^2 l_s^2 / \tilde{v}_1^2 (4 \ln 2)]}{1 + \omega^2 \tau_s^2 (1 - \tilde{v}_1 / c_\infty \cos \varphi)^2} d\mathbf{y}. \quad (4)$$

The amplitude of the effective source is expressed via the turbulence kinetic energy,

$$\hat{q}_s^2 / c^2 = A^2 (2/3 (\bar{\rho} \kappa))^2 \quad (5)$$

which includes the dimensionless calibration parameter  $A$ .

The acoustic correlation space and time scales,  $l_s$  and  $\tau_s$ , are modelled using the local time-averaged flow and turbulence fields. For example, following the original Tam and Auriault work [13], the standard option is to compute these scales from the turbulent kinetic energy and the dissipation rate,

$$l_s = c_\ell \kappa^{1.5} / \varepsilon, \quad \tau_s = c_\tau \kappa / \varepsilon, \quad (6)$$

An alternative option, suggested in [13], is to compute the same quantities from the turbulent kinetic energy and the meanflow vorticity magnitude,

$$l_s = c_\ell \sqrt{\kappa} / \xi, \quad \tau_s = c_\tau / \xi. \quad (7)$$

As discussed in [19], the latter is a preferred option in case the turbulence fields are obtained from LES. Indeed, the direct calculation of the dissipation rate from the definition based on the instantaneous velocity strain rate [45] is challenging, while the consistency of computing the turbulence dissipation by assuming equilibrium of the turbulence dissipation and production terms, applying the RANS-type approach for large eddies, can be debated.

Table A1 summarises calibration parameters suggested in the original publication by Tam and Auriault [13] and the same model implemented by Morris and Farassat [22]. Both of these implementations were based on RANS and the acoustic scales derived using the turbulent energy dissipation rate, (6). Tables A1 and A2 summarise the dimensionless calibration parameters of the current implementation of Tam and Auriault's model, which were obtained for the cold and the hot SILOET jets considered in Table 1. The parameters were obtained by the best fit of the numerically obtained noise spectra to the far-field data from the experiment at a 90° observer angle. Both the LES and RANS meanflow models were used to provide input for the acoustic scale definitions in (6) and (7).

Notably, the parameters obtained for the dimensionless acoustic length and time scales based on the turbulent kinetic energy and the dissipation rate by the best fit for the cold SILOET jet case are within the variation range of the parameters in the previous RANS-based implementations of the same model in [13] and [22]. In addition, some variability of the acoustic scales for the cold and the hot jet is noted. At the same time, the amplitude coefficient is identical for all implementations of Tam and Auriault's model. Furthermore, the acoustic scale parameters based on the LES and RANS meanflow and turbulence fields are reasonably close to each other for the acoustic scale model based on the dissipation rate and, separately, for the model based on the meanflow vorticity, (6) and (7), respectively. The latter suggests that modification of the RANS turbulence model, which was used in the current work following [41] to mimic the LES meanflow solution worked well.

## B. Khavaran's jet noise model

In comparison with Tam and Auriault's model, Khavaran's model includes both the momentum and the fluctuating enthalpy source terms of the Euler equations. By neglecting the correlation between the two different source terms, the far-field noise spectral density of Khavaran's model is computed as a sum of the contributions due to the momentum source  $F_C$  (similar to Tam and Auriault's model) and the fluctuating enthalpy source  $F_H$ ,

$$S_K(\mathbf{x}, \omega) = B_C F_C + B_H F_H, \quad (8)$$

where  $B_C$  and  $B_H$  are dimensionless weight coefficients corresponding to the momentum and enthalpy source terms, which correspond to the cold and hot jet noise sources, respectively.

The momentum and enthalpy source terms of the Khavaran model are

$$F_C = |\cos^2 \varphi + Q \sin \varphi|^2 F, \quad F_H = (1 - M \cos \varphi)^2 \frac{15 c_\infty^2 \overline{h_t'^2}}{16 \kappa \overline{h^2}} F, \quad (9)$$

where

$$F = \frac{\rho_\infty^2 \Upsilon k^4 (1 - M \cos \varphi)^2 |\cos^2 \varphi + Q \sin \varphi|^2}{(4\pi R)^2 (1 - M_c \cos \varphi)^2} \sum_{n=0}^{\infty} (1 + \delta_{0n}) f_n f_n^*, \quad (10)$$

wherein the amplitude coefficient  $f_n$  for each azimuthal mode number  $n$  is a function of radius and obtained numerically as a solution to the second-order ordinary-differential problem [19],

and,

$$Q = \sqrt{\frac{\rho}{\rho_\infty} (1 - M \cos \varphi)^2 - \cos^2 \varphi}. \quad (11)$$

One feature of Khavaran's model, which distinguishes it from Tam and Auriault's model is the empirical model of the convective velocity  $U_c$ ,

$$U_c = a\tilde{v}_1(x, r) + bU_j \quad (12)$$

which involves additional calibration coefficients,  $a \geq 0$  and  $b \geq 0$ .

Another feature of Khavaran's model is the effective source function,  $\Upsilon$ ,

$$\Upsilon(\mathbf{y}, \omega) = \frac{4l_s^3}{5\pi^2} \tilde{v}_1^4 H(\omega_s) N(Z), \quad (13)$$

which, similar to Tam and Auriault's model, agglomerates the directivity effects of all individual source components in a single term. This term includes the more-or-less standard multiplier function,

$$H(\omega_s) = \frac{\tau_s}{1 + (\omega_s \tau_s / 2)^2}, \quad \omega_s = (1 - M_c \cos \varphi) \omega, \quad (14)$$

similar to the multiplier factor of Tam and Auriault's model (4), which appears from the integration over the time delay,  $\tau$  and includes an empirical function, the so-called non-compactness factor,

$$N(Z) = \frac{5}{8(Z)^5} \left( 3 \arctan(Z) - (Z) \frac{5(Z)^2 + 3}{(1 + (Z)^2)^2} \right), \quad Z = (c_l / c_\tau)(\omega \tau_s)(\kappa / c_\infty). \quad (15)$$

The non-compactness factor was suggested using the NASA jet noise database to represent the behaviour of the two-time two-space auto-correlation function more accurately in comparison with the analytical Gaussian-exponential function (3). The argument of the non-compactness factor,  $Z$  increases for large frequencies, thereby leading to an increased contribution for high frequencies compared to using the Gaussian-exponential function [17]. It can also be noted that, in comparison with Tam and Auriault's model, the source amplitude of Khavaran's model is scaled on the axial component of the local jet meanflow velocity rather than turbulent kinetic energy.

In addition, Khavaran's model approximates the fluctuating enthalpy term using another empirical function,

$$\overline{h_i'^2} / \widetilde{h^2} \sim F_T \text{ calibrated on the hot jet noise NASA data [17, 25],}$$

$$F_T = \left( \left| \frac{dT}{dr} \right| \frac{D_j}{T_\infty} \right)^\zeta \frac{(1 - 1/\text{NTR})^\delta}{6} \chi, \quad \chi = \begin{cases} \chi_0 + (1 - \chi_0)t, & z \leq 1, \\ 1, & z > 1, \end{cases} \quad (16)$$

where  $z = y_1 / L_c$ ,  $L_c$  is the length of the potential core of the jet,  $\zeta = 0.2$ ,  $\chi_0 = 0.7$ ,  $\delta = 1 + 1/(3\text{NPR})$ , and where NPR and NTR are the nozzle pressure and temperature ratios, respectively.

Similar to Tam and Auriault's model, the correlation space and time scales of Khavaran's model are reconstructed from the local time-averaged flow quantities, using (6) or (7).

Table A1 summarises the calibrations parameters of Khavaran's model suggested in the original publication by [23], which were based on RANS and the acoustic scale formulation using the turbulent energy dissipation rate, (6). Tables A1 and A2 summarise the calibration parameters of the current implementation of Khavaran's model based on the best fit to the far-field noise experiment data at the 90° observer angle. This is same angle as selected for the Tam and Auriault model in Section A. Notably, acoustic model calibrations based on the far-field data are preferred at this particular angle in order to make the calibration procedure less dependent on the meanflow refraction effects, which are negligible at 90° to the jet axis.

Both the LES and RANS solutions are applied for the acoustic scale models (6) and (7). Unlike a Tam and Auriault's model in Section A, here we were unable to obtain dimensionless calibration parameters of the implemented Khavaran's model for the SILOET jet close to the recommended set of values from the original publication [23]. The difference in the coefficients may be attributed to a greater sensitivity of Khavaran's model to jet experiment in comparison with that of Tam and Auriault's model, which has a smaller number of calibration parameters. Furthermore, the dimensionless amplitude coefficients of the fluctuating momentum and enthalpy source terms of Khavaran's model (which were not reported in the original publication [23]) are quite sensitive to the jet temperature as well as the meanflow and turbulence modelling (RANS vs. LES). At the same time, the variability of the acoustic length and time scale parameters of Khavaran's model from the cold jet to the hot jet is similar compared to that of Tam and Auriault's model in Section A (comp. Tables A1 and A2 for the implementation of Tam and Auriault's model and Khavaran's model).

### C. The Generalised Acoustic Analogy model for hot jet noise

In comparison with Khavaran's model, the current implementation of the Goldstein Generalised Acoustic Analogy (GAA) considers the effective source terms in the laboratory frame, while keeping the individual

directivities of the fluctuating Reynolds stress components and enthalpy terms. By computing the acoustic integral as an inner product of the individual source terms and the components of the vector adjoint Green's function, the model captures the total jet noise directivity for a wide range of observer angles including the side-line and the peak jet noise angles [46].

Following [19, 26-28], after a series of re-arrangements, which include shifting the derivatives from the source to the Green's function propagator operator via the integration by parts and, similar to the Khavaran's model, neglecting the correlation between the different source terms, the expression for the far-field noise spectra becomes:

$$S_G(\mathbf{x}, \omega) = S_C + S_H, \quad (17)$$

where

$$S_C(\mathbf{x}, \omega) = \int_V \int_V \hat{R}_{ijkl}(\mathbf{y}, \Delta, \omega) \hat{I}_{ij}(\mathbf{y}, \omega | \mathbf{x}) \hat{I}_{kl}^*(\mathbf{y} + \Delta, \omega | \mathbf{x}) d(\Delta) d\mathbf{y}, \quad (18)$$

and

$$S_H(\mathbf{x}, \omega) = \int_V \int_V \hat{H}_{ij}(\mathbf{y}, \Delta, \omega) \hat{I}_i(\mathbf{y}, \omega | \mathbf{x}) \hat{I}_j^*(\mathbf{y} + \Delta, \omega | \mathbf{x}) d(\Delta) d\mathbf{y}, \quad (19)$$

wherein  $S_C$  and  $S_H$  correspond to contributions of the fluctuating momentum and enthalpy source terms of the linearised Euler equations, respectively,  $i, j, k, l$  are Cartesian coordinate indices each of which varies from 1 to 3 ( $e_1$  is in the jet stream direction and  $e_2, e_3$  are the other two Cartesian components in the jet-normal plane), and

$$\begin{aligned} \hat{I}_{ij}(\mathbf{y}, \omega | \mathbf{x}) = & \frac{\partial \hat{v}_j^{(a)}(\mathbf{y}, \omega | \mathbf{x})}{\partial y_i} - \left[ \frac{\partial \tilde{v}_j}{\partial y_i}(\mathbf{y}) p^{(a)}(\mathbf{y}, \omega | \mathbf{x}) + \tilde{v}_j \frac{\partial p^{(a)}(\mathbf{y}, \omega | \mathbf{x})}{\partial y_i} \right] \\ & + \frac{\delta_{ij}}{2} \left( i\omega + \tilde{v}_k \frac{\partial}{\partial y_k} \right) p^{(a)}(\mathbf{y}, \omega | \mathbf{x}), \end{aligned} \quad (20)$$

and

$$\hat{J}_i(\mathbf{y}, \omega | \mathbf{x}) = -\frac{\partial p^{(a)}(\mathbf{y}, \omega | \mathbf{x})}{\partial y_i}. \quad (21)$$

are the Green's function propagator operators corresponding to the fluctuating momentum and enthalpy source terms, respectively.

The acoustic integrals include the time-domain Fourier transforms of the corresponding fluctuating Reynolds stress and enthalpy terms,

$$\hat{R}_{ijkl}(\mathbf{y}, \Delta, \omega) = \int_{-\infty}^{\infty} R_{ijkl}(\mathbf{y}, \Delta, \tau) e^{i\omega\tau} d\tau, \text{ and } \hat{H}_{ij}(\mathbf{y}, \Delta, \omega) = \int_{-\infty}^{\infty} H_{ij}(\mathbf{y}, \Delta, \tau) e^{i\omega\tau} d\tau. \quad (22)$$

Here «\*» denotes complex conjugate and the corresponding covariance functions are

$$R_{ijkl}(\mathbf{y}, \Delta, \tau) = \overline{T'_{ij}(\mathbf{y}, t) T'_{kl}(\mathbf{y} + \Delta, t + \tau)}, \quad H_{ij}(\mathbf{y}, \Delta, \tau) = \overline{H'_i(\mathbf{y}, t) H'_j(\mathbf{y} + \Delta, t + \tau)}, \quad (23)$$

$$T'_{ij} = -\left(\rho v'_i v'_j - \overline{\rho v'_i v'_j}\right), \quad H'_i = -\left(\rho v'_i h'_0 - \overline{\rho v'_i h'_0}\right),$$

where further details of the GAA implementation can be found in [19].

For simplicity, following Tam and Auriault's model, the covariance of fluctuating Reynolds stresses in (18) are approximated by the Gaussian-exponential model

$$R_{ijkl}(\mathbf{y}, \Delta, \tau) = A_{ijkl}(\mathbf{y}) \exp\left[-\frac{|\Delta_1|}{\tilde{v}_1 \tau_s} - \frac{\ln 2}{l_s^2} \left((\Delta_1 - \tilde{v}_1 \tau)^2 + \Delta_2^2 + \Delta_3^2\right)\right]. \quad (24)$$

Following Khavaran [17, 25], the covariance of the fluctuating enthalpy term in (19) is represented by a product of the velocity auto-correlation function and the fluctuating enthalpy function

$$\hat{H}_{ij}(\mathbf{y}, \Delta, \omega) = \hat{R}_{ij}(\mathbf{y}, \Delta, \omega) \overline{h'_i{}^2} / \tilde{h}^2, \quad (25)$$

where the former,

$$R_{ij}(\mathbf{y}, \Delta, \tau) = \overline{v'_i(\mathbf{y}, t) v'_j(\mathbf{y} + \Delta, t + \tau)} \quad (26)$$

is approximated by the Gaussian-exponential model by analogy with the co-variance of fluctuating Reynolds stresses,

$$R_{ij}(\mathbf{y}, \Delta, \tau) = A_{ij}(\mathbf{y}) \exp\left[-\frac{|\Delta_1|}{\tilde{v}_1 \tau_s} - \frac{\ln 2}{l_s^2} \left((\Delta_1 - \tilde{v}_1 \tau)^2 + \Delta_2^2 + \Delta_3^2\right)\right]. \quad (27)$$

and the latter factor

$$\overline{h'_i{}^2} / \tilde{h}^2 = F_T \quad (28)$$

is further expressed as a function of the temperature gradient following Khavaran and Bridges, (16).

The final expression for the momentum (18) and fluctuating enthalpy (19) parts of the far-field noise spectra are given by

$$S_C = \int_V \int_V A_{ijkl}(\mathbf{y}) W(\mathbf{y}) \hat{I}_{ij} \hat{I}_{kl}^* d\mathbf{y}, \text{ and } S_H = \int_V \int_V A_{ij}(\mathbf{y}) W(\mathbf{y}) \hat{J}_i \hat{J}_j^* d\mathbf{y}, \quad (29)$$

where the function  $W(\mathbf{y})$ , which appears from evaluating the integrals over the correlation volume  $\Delta$  analytically similar to Tam and Auriault's model, is:

$$W(\mathbf{y}) = \left( \frac{\pi}{\ln 2} \right)^{3/2} \frac{2l_s^3 \tau_s}{1 + (\omega(1 - \tilde{v}_1 / c_\infty \cos \varphi) \tau_s)^2} \exp\left( -\frac{(\omega l_s / \tilde{v}_1)^2}{4 \ln 2} \right). \quad (30)$$

Further derivation details can be found in [19].

Similar to Tam and Auriault's model, the amplitudes of the fluctuating momentum and enthalpy source terms are modelled using the turbulent kinetic energy,  $\kappa$ ,

$$A_{ijkl}(\mathbf{y}) = C_{ijkl} (2\bar{\rho}\kappa)^2, \quad A_{ij}(\mathbf{y}) = C_{ij} \rho_\infty c_\infty^4 \bar{\rho}\kappa F_T. \quad (31)$$

The dimensionless coefficients  $C_{ijkl}$  and  $C_{ij}$ ,  $i, j, k, l = 1, 2, 3$  are cylindrical-polar coordinate indices ( $e_1$  is in the jet direction,  $e_2 = e_r, e_3 = e_\theta$ ) were computed from the LES solution along the jet lip-line  $r / D_j = 0.5$ . The computation details can be found in [19]. Briefly, the non-dimensional amplitude parameters in (31) are given as

$$C_{ijkl} = \langle \alpha_{ijkl} \rangle \alpha_0, \quad C_{ij} = \langle \beta_{ij} \rangle \beta_0, \quad (32)$$

where  $\langle \cdot \rangle$  stands for the spatial averaging over the jet lip-line locations from the early shear layers to the end of the jet potential core. The distributions of several most significant components were computed as

$$\alpha_{ijkl}(y_1) = \frac{R_{ijkl}(y_1)}{\max(R_{1111})}, \quad \beta_{ij}(y_1) = \frac{R_{ij}(y_1)}{\max(R_{11})}, \quad (32)$$

where the maximum is taken over all jet lip-line locations, and all amplitudes are scaled on the turbulent kinetic energy,

$$\alpha_0 = \frac{R_{1111}(y_1)}{(2\bar{\rho}\kappa)^2}, \quad \beta_0 = \frac{R_{11}(y_1)}{\bar{\rho}\kappa}. \quad (32)$$

The resulting dimensionless amplitude parameters of the major source components are provided in Tables 4 and 5. Notably, it was previously shown (fig.15 in [38]) that the 5 major relative amplitudes  $\alpha_{ijkl}$  corresponding to  $(rr, rr)$ ,  $(\theta\theta, \theta\theta)$ ,  $(1r, 1r)$ ,  $(1\theta, 1\theta)$ , and  $(r\theta, r\theta)$  correlation amplitudes in Table 4 only weakly depend on the LES case, when measured in the outer shear layers of co-axial jets, where the latter behave similar to single-stream in

terms of jet noise. Therefore, it can be assumed that the dimensionless amplitude parameters remain approximately constant for a class of single-stream jet cases.

Tables A1 and A2 summarise the acoustic length and time scale parameters, which were obtained by the best fit to the far-field experiment data at 90° observer angle, in the same manner as for the other two acoustic models described in Sections A and B. The acoustic length and time scale calibration parameters of the GAA model show more-or-less similar sensitivity to the jet temperature and the choice of the meanflow and turbulence model as the Tam and Auriault and the Khavaran models.

**Table 4. Amplitude parameters of the GAA model for the fluctuating momentum source term**

| $C_{ijkl}$      | 11,11 | $rr,rr$ | $\theta\theta,\theta\theta$ | $1r,1r ; 1r,r1;$ | $1\theta,1\theta ; 1\theta,\theta 1;$  | $r\theta,r\theta ; \theta r,r\theta ; \theta r,\theta r$ |
|-----------------|-------|---------|-----------------------------|------------------|--|--|
|                 |       |         |                             | $r1,1r ; r1,r1;$ | $\theta 1,1\theta ; \theta 1,\theta 1$ | $; r\theta,\theta r$                                     |
| Cold SILOET jet | 1     | 0.355   | 0.360                       | 0.327            | 0.326                                  | 0.180  |
| Hot SILOET jet  | 1     | 0.360   | 0.369                       | 0.329            | 0.331                                  | 0.183  |

**Table 5. Amplitude parameters of the GAA model for the fluctuating enthalpy source term**

| $C_{ij}$        | 11 | $rr$  | $\theta\theta$ | $1r$  | $1\theta$ | $r\theta$ |
|-----------------|----|-------|----------------|-------|-----------|-----------|
| Cold SILOET jet | 1  | 0.586 | 0.330          | 0.331 | 0         | 0         |
| Hot SILOET jet  | 1  | 0.453 | 0.257          | 0.259 | 0         | 0         |

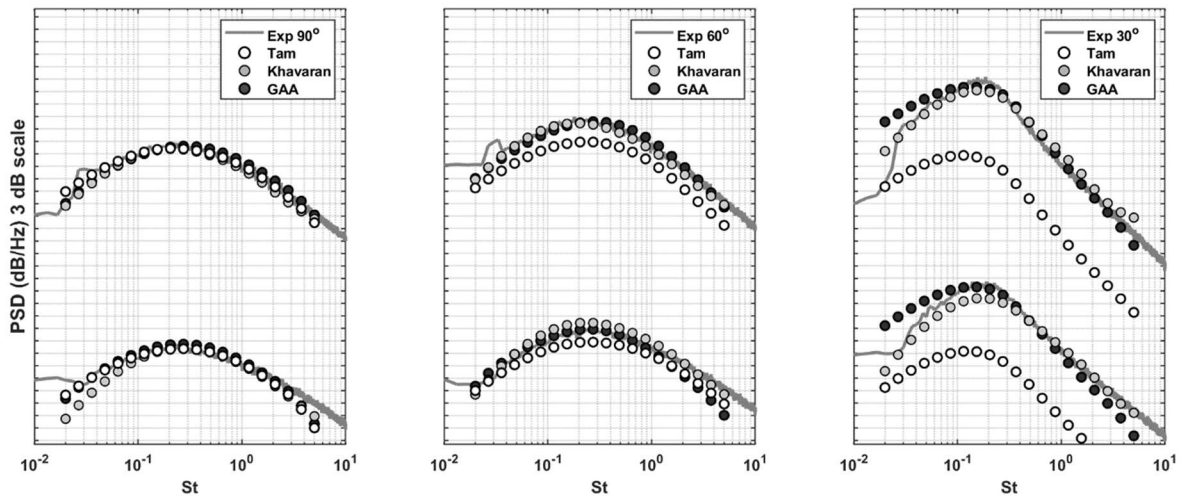
## IV. Results of the Acoustic Modelling

### A. Performance of the acoustic models for the cold and hot SILOET jets

Figs. 3-4 show the acoustic spectra predictions of the three models using the standard definition of acoustic scales based on the turbulent kinetic energy and the dissipation rate (6).

The far-field noise spectra predictions based on the RANS solutions are compared first (Fig.3). As expected, Tam and Auriault's model captures the noise spectra shape of the SILOET jets at the observer angle 90° very well, within 1 dB from the experiment for all frequencies within  $0.03 < St_D < 4$ . The model predictions start to deteriorate

at the intermediate angle of  $60^\circ$  to the jet flow especially for the hot jet (4 dB error) and completely fail to capture the peak jet noise at a  $30^\circ$  observer angle (14-15 dB error), which is not surprising given the isotropic nature of the fine-scale turbulence noise model. In comparison with Tam and Auriault's model, Khavaran's model predicts noise within 2-3 dB for both the cold and the hot jets for all observer angles including the peak noise at  $30^\circ$  angle. Khavaran's model does not capture the shape of the noise spectrum for the  $90^\circ$  observer angle for low frequencies compared to the Tam model, however, the overall agreement with the experiment is good for the frequency range  $0.03 < St_D < 4$  especially for the hot jet (within a 2 dB error). The improved agreement with hot jet can be explained by the explicit modelling of the enthalpy noise as well as the large number of calibration parameters in comparison with Tam and Auriault's model. However, it remains unclear if all these calibration parameters can be supported by experimental observations. For example, we find that for obtaining good predictions for the considered SILOET jets with Khavaran's model one needs to set the convective velocity to  $U_c \sim 0.8U_j$ . The latter scaling is notably higher compared to the value,  $U_c \sim 0.65U_j$ , which was previously reported in the experiment [47]. In addition, the recommended set of parameters of Khavaran's model originally suggested in [23, 24] (Table A1) leads to a large offset of the predicted noise spectra in comparison with the experiment. The GAA model captures the noise spectra within 2 dB for most frequencies and all three observer angles. It captures the peak jet noise of the cold SILOET jet for  $60^\circ$  and  $30^\circ$  observer angles within 0.5dB while Khavaran's model shows some 3 dB underprediction of the peak noise. For the hot SILOET jet, the predictions of the GAA model and Khavaran's model are similar for all angles apart from low frequencies at  $30^\circ$ , where the GAA model is less accurate for low frequencies.



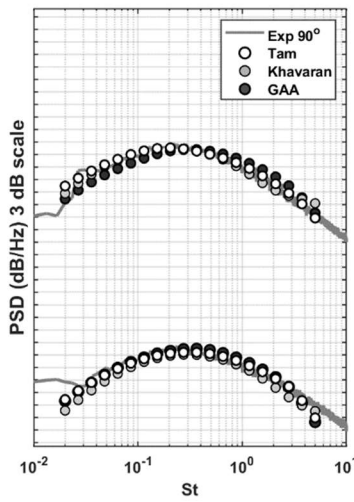
(a)

(b)

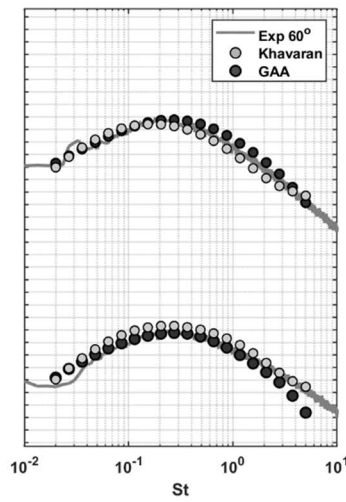
(c)

**Fig. 3 Noise spectra predictions of the cold (bottom) and hot (top) SILOET jet using the correlation scales based on the turbulent kinetic energy and dissipation rate reconstructed from RANS: comparison of the Tam and Auriault, Khavaran, and GAA models with the experiment for 90° (a), 60°(b), and 30° (c) observer angles. The unit scale on the PSD axis is 3dB.**

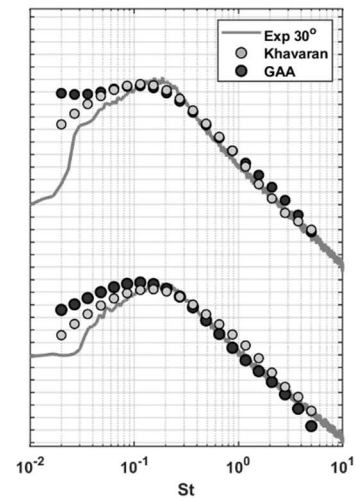
Fig.4 compares the predictions of the same jet noise models when the RANS solutions are replaced by the LES fields. Far-field noise results of the Tam and Auriault model at 90° are insensitive to the change of the input flow data within a small modification of the model parameters. A more significant change of the calibration parameters of Khavaran’s model has been required to preserve a good agreement with the experiment when the RANS input is replaced by LES. This change also included a recalibration of the effective convection speed,  $U_c$ . Notably, with the LES input, Khavaran’s model leads to a more accurate prediction of the peak noise level at the 30° observer angle for the cold SILOET jet in comparison with the RANS-based results (comp. Fig.4 with Fig.3). Similar to Khavaran’s model, the GAA model also required a readjustment of the source parameters to match the 90° observer spectra for the cold and hot SILOET jets with the LES input (Table 5). For the cold jet case, overall, the predictions of the GAA model implementation [19] based on the LES data are more-or-less similar to those of Khavaran’s model. However, the results of the LES-based GAA model for the hot jet at 30° show a strong amplification at low frequencies, where a spurious second peak begins to emerge. As discussed in [19], this spurious amplification is an artefact of using the dissipation rate in the definition of the acoustic length and time scales of the GAA model.



(a)



(b)



(c)

**Fig. 4 Noise spectra predictions of the cold (bottom) and hot (top) SILOET jet using the correlation scales based on the turbulent kinetic energy and dissipation rate reconstructed from LES: comparison of the Tam and Auriault, Khavaran, and GAA models with the experiment for 90° (a), 60°(b), and 30° (c) observer angles. The unit scale on the PSD axis is 3dB.**

The next series of Figs.5-6 compare the predictions of the three acoustic models when using the turbulent kinetic energy and the meanflow vorticity as the local flow quantities to compute the acoustic correlation scales (7). This choice of acoustic scale models avoids using the turbulent kinetic energy dissipation rate and appears to be more suitable for the LES data.

Fig.5 show the results for the RANS-based acoustic models and Fig.6 show the results of acoustic predictions using the LES input. Again, at 90° Tam and Auriault’s model is virtually insensitive to the choice of the RANS or LES input data. Similar to the standard option of using the correlation scales normalised by the turbulence kinetic energy and dissipation rate (Figs. 3-4), the model captures the 90° noise spectrum shape very well (~1 dB). The performance of Khavaran’s model for the acoustic scales based on the meanflow vorticity is very similar to that using the dissipation rate for the full range of observer angles considered. The RANS-based Khavaran’s model tends to be within 2 dB from the experiment for the hot SILOET jet case while for the cold jet it underpredicts the peak noise at the 30° observer angle and overpredicts noise at 60° angle. The use of the LES dataset, instead of RANS, improves the model accuracy to become within 2 dB from the experiment for both the SILOET jets, similar to the solutions based on the dissipation rate. One exception is the intermediate observer angle of the cold jet where both the LES- and RANS-based Khavaran’s model overpredicts noise by 3 dB (Figs. 5 and 6). The accuracy of the GAA model based on the LES data and the meanflow vorticity to reconstruct the acoustic correlation scales in comparison with the experiment becomes 2 dB for most frequencies, both for the cold and the hot jet (Fig.6). Compared to this, for the RANS-based GAA model, the choice of the acoustic scales based on the meanflow vorticity leads to a shift of the peak noise to a low frequency,  $St_D \sim 0.1$  (Fig.5c).

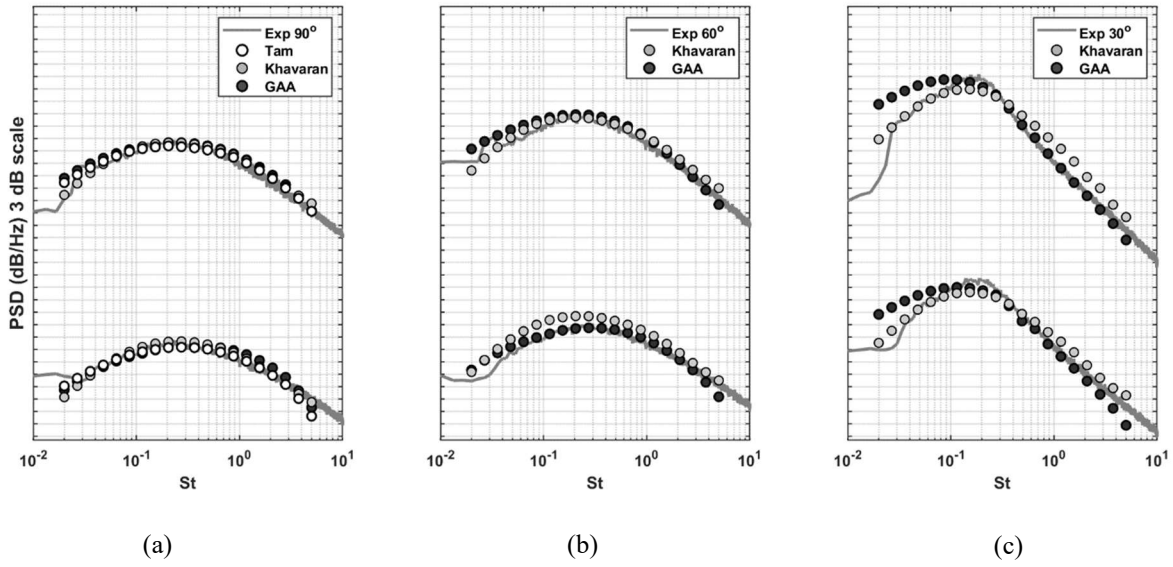


Fig. 5. Noise spectra predictions of the cold (bottom) and hot (top) SILOET jet using the correlation scales based on the turbulent kinetic energy and meanflow vorticity reconstructed from RANS: comparison of the Tam and Auriault, Khavaran, and GAA models with the experiment for 90° (a), 60°(b), and 30° (c) observer angles. The unit scale on the PSD axis is 3dB.

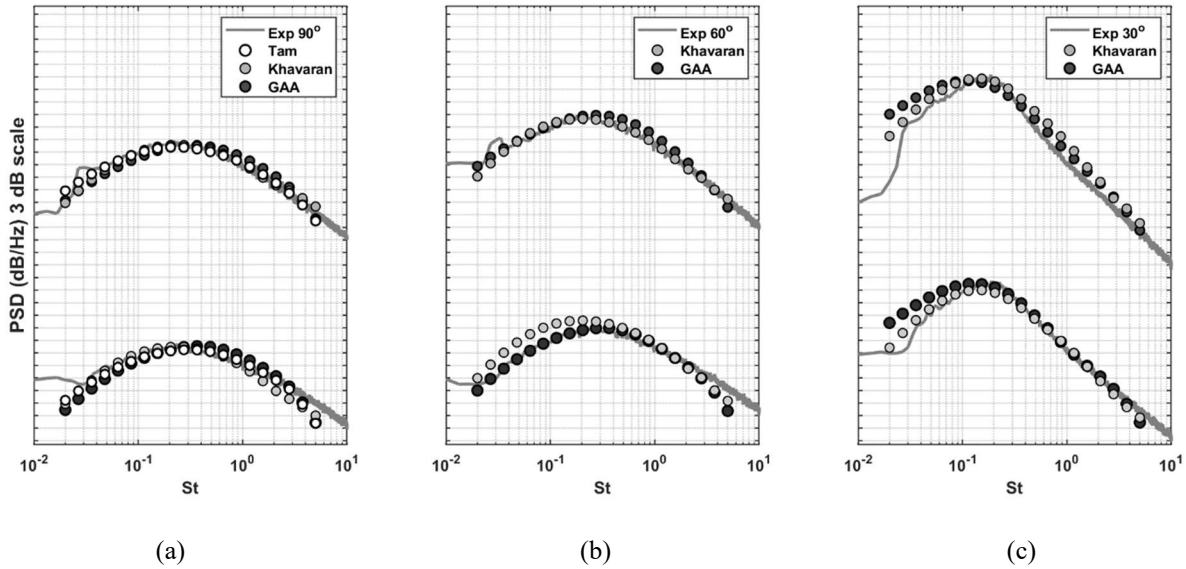
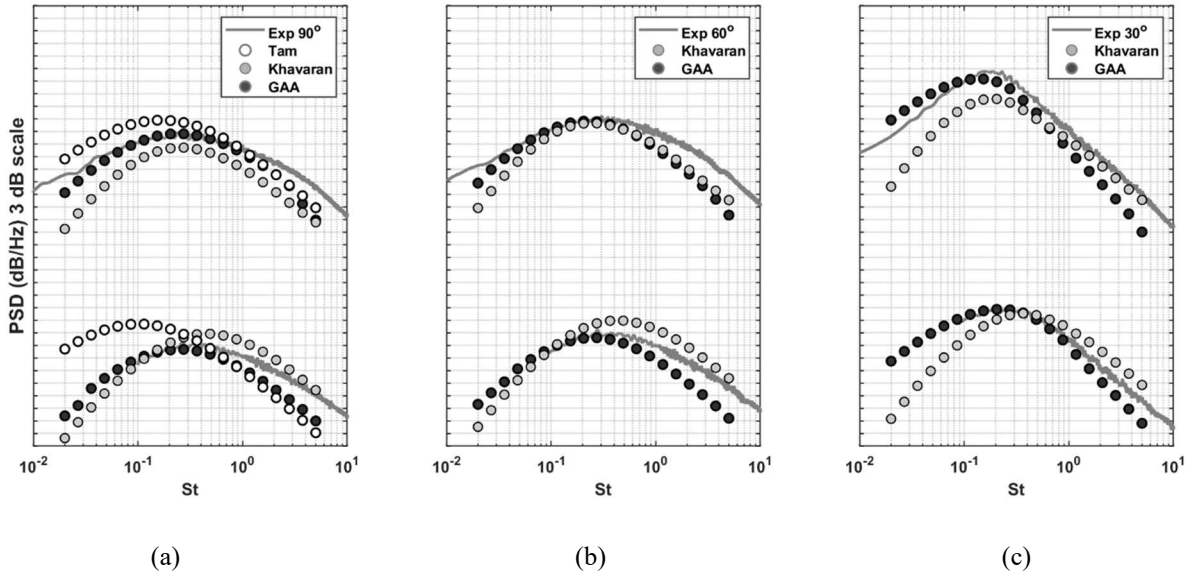


Fig. 6. Noise spectra predictions of the cold (bottom) and hot (top) SILOET jet using the correlation scales based on the turbulent kinetic energy and meanflow vorticity reconstructed from LES: comparison of the Tam and Auriault, Khavaran, and GAA models with the experiment for 90° (a), 60°(b), and 30° (c) observer angles. The unit scale on the PSD axis is 3dB.

## B. Sensitivity of the acoustic source models to a variation of the jet noise experiment

Here, the dimensionless space and time length scale parameters of each of the acoustic models considered in Section A for the cold SILOET jet are applied for far-field noise predictions of the NASA SP3 and SP7 jets using the same models. For input to the acoustic modelling of the NASA jets, the relevant input RANS and LES datasets are used as discussed in Section II.

Figs.7-8 show the noise spectra predictions based on the acoustic length scale definition using the dissipation rate using parameters of the cold SILOET models (Table A1). The RANS-based implementations of Tam and Auriault's and Khavaran's models show an offset of the noise spectra at the peak frequency, thereby leading to 4-5 dB errors at 90° and 60° observer angles (Fig.7). A similar trend is observed for LES-based implementations of the two models (Fig.8). In comparison with Tam and Auriault's and Khavarans models, the GAA model based on the source parameters obtained for the cold SILOET jet manages to produce encouraging results for the NASA SHJAR jets. Notably, the peak jet noise spectra are well captured for all angles and a consistent 2dB accuracy is observed for frequencies up to  $St_D=1-2$ .



**Fig. 7** Noise spectra predictions of the SHJAR SP3 (bottom) and SP7 (top) jets using the correlation scales based on the turbulent kinetic energy and dissipation rate reconstructed from RANS with dimensionless parameters of the cold SILOET jet model: comparison of the Tam and Auriault, Khavaran, and GAA models with the experiment for 90° (a), 60°(b), and 30° (c) observer angles. The unit scale on the PSD axis is 3dB.

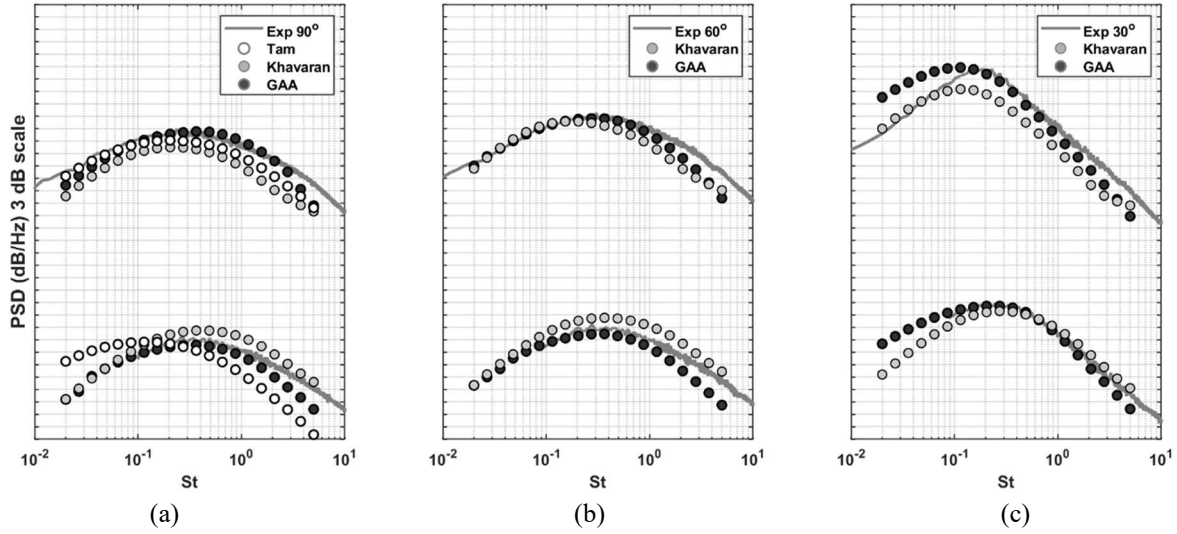


**Fig. 8** Noise spectra predictions of the SHJAR SHJAR SP3 (bottom) and SP7 (top) jets using the correlation scales based on the turbulent kinetic energy and dissipation rate reconstructed from LES with dimensionless parameters of the cold SILOET jet model: comparison of the Tam and Auriault, Khavaran, and GAA models with the experiment for 90° (a), 60°(b), and 30° (c) observer angles. The unit scale on the PSD axis is 3dB.

Figs. 9-10 show the noise spectra predictions using the acoustic length scale definition based on the meanflow vorticity while using the parameters obtained earlier for the cold SILEOT models (Table A2). The results of Tam and Auriault’s model show a large underprediction of noise for all angles and both the NASA jet cases. The noise predictions of Khavaran’s model show reasonably good predictions for the NASA SP7 jet using both the RANS (Fig.9) and the LES datasets (Fig.10) at 90 and 60° observer angles. However, its peak noise predictions at 30° are attenuated by 5-6 dB. It can be noted that the NASA SP7 jet is most similar to the cold SILOET jet case. In comparison with this, the results of Khavaran’s model for the NASA SP3 jet, which has a different Mach number, remain poor: the model fails to capture the sound amplification depending on the observer angle (Figs. 9 and 10). At the same time, the GAA noise predictions show good accuracy and the correct location of the peak frequency in comparison with the NASA data in all cases. For the LES-based flow fields, the GAA predictions of the NASA SP3 and SP7 jet noise are especially good: the error from the experiment is within 2 dB up to  $St_D=2-3$  (Figs.17-18), which accuracy is comparable to the results of the GAA model for the cold SILOET jet (Fig.6).

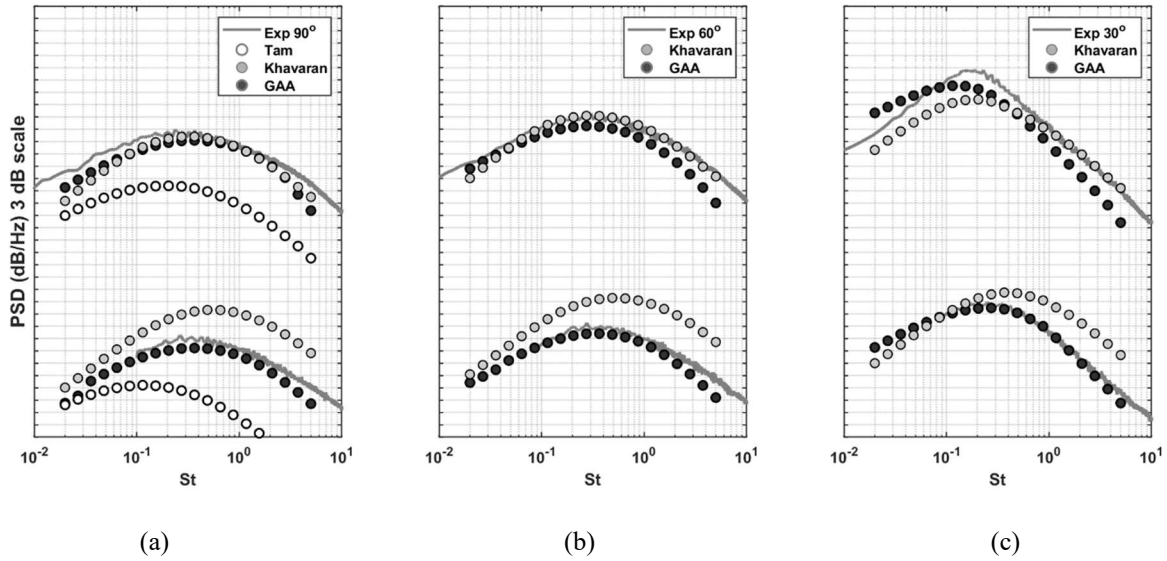


**Fig. 9** Noise spectra predictions of the SHJAR SP3 (bottom) and SP7 (top) jets jet using the correlation scales based on the turbulent kinetic energy and meanflow vorticity reconstructed from RANS with dimensionless parameters of the cold SILOET jet model: comparison of the Tam and Auriault, Khavaran, and GAA models with the experiment for 90° (a), 60°(b), and 30° (c) observer angles. The unit scale on the PSD axis is 3dB.

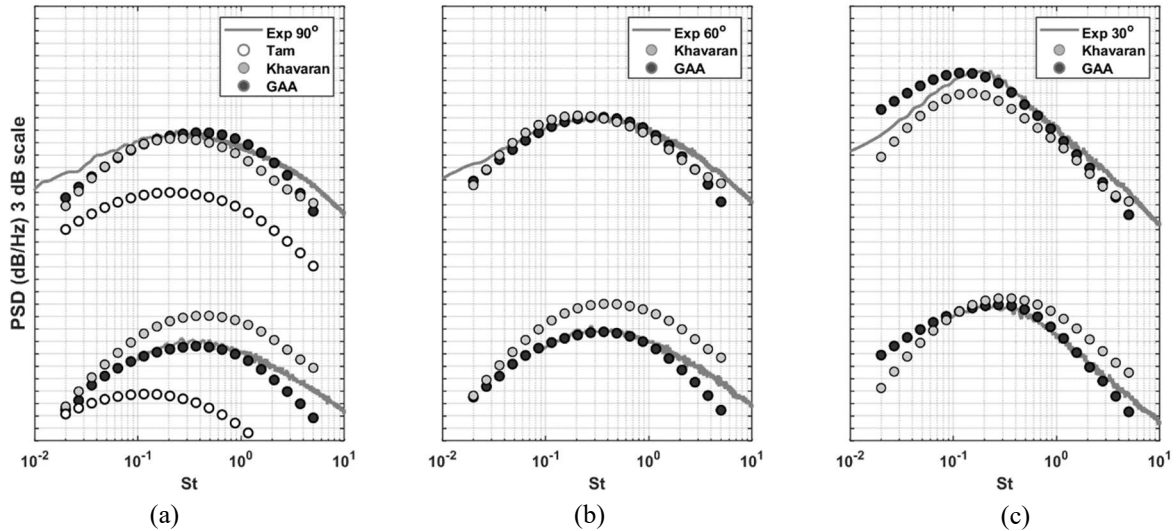


**Fig. 10** Noise spectra predictions of the SHJAR SP3 (bottom) and SP7 (top) jets jet using the correlation scales based on the turbulent kinetic energy and meanflow vorticity reconstructed from LES with dimensionless parameters of the cold SILOET jet model: comparison of the Tam and Auriault, Khavaran, and GAA models with the experiment for 90° (a), 60°(b), and 30° (c) observer angles. The unit scale on the PSD axis is 3dB.

### C. Sensitivity of acoustic results to a choice of the baseline jet experiment

It can be argued that the results of the acoustic models considered in Section B, such as Tam and Auriault's and Khavaran's, showed the largest sensitivity to a variation of the jet conditions, depending on the definition of the reference jet experiment. Hence, here we consider the NASA SP7 jet as the new anchoring point to calibrate Tam and Auriault's model, similar to how its calibration was performed in the original publication [13]. Following the procedure outlined in Section III, the meanflow and turbulence fields from the RANS and LES are used to compute the acoustic scales and the source amplitude, while the corresponding dimensionless parameters are obtained from the best fit to the far-field noise experiment data from NASA at 90° observer angle. The corresponding dimensionless scales and amplitude coefficients for acoustic scales based on the dissipation rate and the meanflow vorticity are summarised in Tables A1 and A2. As expected, the dimensionless parameters obtained for the RANS input data and the acoustic scales based on the dissipation rate have turned out to be the same as originally suggested in [13] (Table A1), which used the same RANS-based model. Fig. 11 shows the obtained results with the far-field spectra measurements using the RANS and LES solutions based on the two definitions of the acoustic scales. Notably, similar to the previous noise predictions for the SILOET jets (Fig.3-6), the agreement of most implementations of Tam and Auriault's model with the NASA data is within 1 dB for all frequencies at 90° observer angle and quickly deteriorates for smaller angles, away from the validity range of the fine-scale jet mixing noise model.

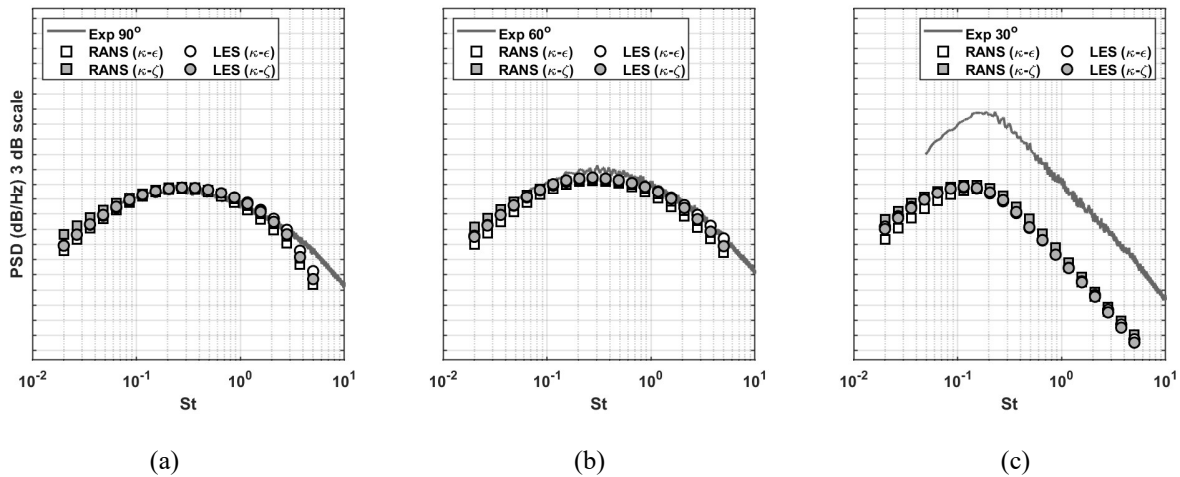


**Fig. 11 Noise spectra predictions of the SHJAR SP7 jet using Tam and Auriault' model: comparison of the RANS- and LES-based acoustic predictions for dissipation rate- and vorticity-based acoustic scales with the experiment for 90° (a), 60°(b), and 30° (c) observer angles. The unit scale on the PSD axis is 3dB.**

Having calibrated the implementation of Tam and Auriualt’s model on the NASA jet, the same dimensionless acoustic scale parameters are applied to predict the noise of the cold SILOET jet using the suitable RANS and LES solutions from Section A. The results are demonstrated in Fig.12. Not to mention the expected underprediction of the peak jet noise at 30°, the results also show a 5 dB noise amplification at 90° and 60° angles and a shift of the peak jet frequency in comparison with the SILOET experiment even at 90° angle. This re-confirms a strong sensitivity of parameters of Tam and Auriualt’s jet noise model to the jet experiment on the considered set of two SILOET and two NASA jet cases.

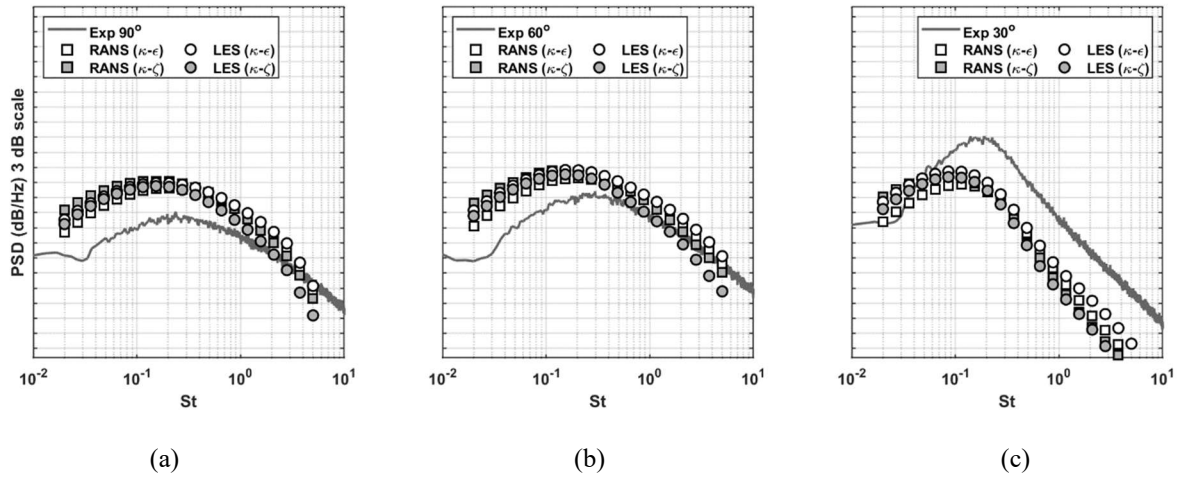


**Fig. 12 Noise spectra predictions for the cold SILOET jet using Tam and Auriualt’s model using the dimensionless parameters computed from the NASA SP7 jet model: comparison of the RANS- and LES-based acoustic predictions for dissipation rate- and vorticity-based acoustic scales with the experiment for 90° (a), 60°(b), and 30° (c) observer angles. The unit scale on the PSD axis is 3dB.**

## V.Conclusion

Three well-established reduced-order jet noise models are compared on a set of four single stream jet cases corresponding to a range of the jet temperature and velocity conditions. Two of the cases correspond to the cold and hot SILOET jets at the same acoustic Mach number of 0.875 in the experiment performed by QinetiQ. The other two cases correspond to the cold jets of the NASA SHJAR experiment, where the acoustic Mach number varies from 0.5 to 0.9. The idea behind this comparison is to cross-verify the robustness of the reduced-order models to a variation of the baseline jet case used for calibration of the acoustic source parameters. The models are tested to the choice of the input flow and turbulence data (RANS vs. LES flow fields) as well as the modelling of the acoustic length and time scales via the single-point time-averaged flow data, for which a few options exist such as using turbulent

kinetic energy and dissipation rate or meanflow vorticity. The compared models are implementations of Tam and Auriault's, Khavaran's, and the Goldstein Generalised Acoustic Analogy (GAA) jet noise prediction schemes. The models are different depending on the total number of model calibration parameters (smallest in the Tam and Auriault's case) and by the number of the calibration parameters to be adjusted based on the far-field noise data (smallest in the GAA case). In comparison with the other acoustic models, the effective source of the GAA model is computed in the laboratory nozzle frame by removing the material derivative from the fluctuating turbulent sources. This allowed using relative amplitudes of the individual source components extracted from a previous single-stream jet calculation. Hence, the number of adjustable parameters of the GAA model is two, as the number of parameters used in the acoustic space and time scales model.

In the first step, all three models are applied for conditions of the cold and hot SILOET jets with performing individual source parameter calibrations in each case. The fine-scale jet mixing noise model of Tam and Auriault predicts noise within 1 dB for 90° observer angle, however, its predictions quickly deteriorate for angles away from the side-line observer position. The implementations of Khavaran's and the GAA model show more-or-less similar accuracy within 2 dB from the experiment up to frequencies  $St_D \sim 4-5$ , depending on the jet case, observer angle, and frequency and the choice of the meanflow and turbulence model. The results obtained using the LES data tend to be more accurate compared to the RANS-based solutions.

In the next step, the sensitivity of the acoustic models to a variation from the cold SILOET jet conditions is analysed. For this purpose, the dimensionless source model parameters obtained for the cold SILOET jet flow are applied for predicting the noise of the NASA SP3 and SP7 jets. In each case, suitable RANS and LES flow solutions of the NASA jets are used in the acoustic modelling based on the dissipation rate or meanflow vorticity choices. The results show large errors for the implemented Tam and Auriault's and Khavaran's models especially for the NASA SP3 jet, where both models have problems to correctly predict noise even at a 90° angle. In comparison with this, the accuracy of the GAA model remains fairly good especially in the case of using the LES dataset and the acoustic scale definition based on the meanflow vorticity. In the latter case the GAA model preserves a 2 dB accuracy up to a frequency of  $St_D \sim 2-3$ .

Finally, to examine the sensitivity of the acoustic models showing the greatest sensitivity to a variation of the jet noise case, the implementation of Tam and Auriault's model is re-adjusted for conditions of the NASA SP7 jet and then applied to predict the noise of the cold SILOET jet for the same dimensionless acoustic scale coefficients.

For the input to the acoustic model, the choice of RANS and LES data is considered and so are the two acoustic scale approximations based on the dissipation rate and the meanflow vorticity. In this case, dimensionless parameters of the implemented Tam and Auriat's model coincide with those recommended in the original work, which reconfirms the consistency of the current implementation of the same model. However, the results of the recalibrated Tam and Auriat's model show large differences (~5dB) with the SILOET experiment even for a 90° observer angle.

The main result of this work is that the GAA model is recommended for further investigations and testing towards its use in fast-turn-around multidisciplinary design optimisation studies. Neither Tam and Auriat's model nor Khavaran's model appears to be sufficiently robust for using them in acoustic optimisation.

All acoustic models investigated in this study have been implemented in MATLAB. The MATLAB scripts together with the corresponding input and output data can be downloaded following the link <https://github.com/vasily-gryazev/Jet-Noise>.

### **Acknowledgement**

The authors are grateful to the UK Government for supporting the SILOET program (Innovate UK (former TSB), Reference number 110032) during which the model-scale data was acquired in the QinetiQ NTF and Rolls-Royce Plc for facilitating access to these data.

This work has been supported by Decrease Jet-Installation Noise (DJINN) project (Grant agreement ID: 861438). The work of A.P. Markesteijn and S.A. Karabasov have been supported by the Engineering and Physical Sciences Research Council (EP/S002065/1), and S.A. Karabasov acknowledges the study performed in TsAGI with the financial support provided by the Ministry of Science and Higher Education of the Russian Federation (Grant Agreement of December 8, 2020, No 075-11-2020-023) within the program for creation and development of the World-Class Research Center "Supersonic".

### **References**

- [1] Rallabahndi, S. K., Loubeau, A., "Summary of Propagation Cases of the Second AIAA Sonic Boom Prediction Workshop," *Journal of Aircraft*, Vol. 56-3, 2019. <https://doi.org/10.2514/1.C034805>

- [2] Head, R., and Fisher, M., Jet surface interaction noise - analysis of far-field low frequency augmentations of jet noise due to the presence of a solid shield, 3rd Aeroacoustics Conference, Palo Alto, CA, U.S.A., 1976. <https://doi.org/10.2514/6.1976-502>
- [3] Jordan, P., Jaunet, V., Towne, A., Cavalieri, A.V.G., Colonius, T., Schmidt, O., Agarwal, A., Jet-flap interaction tones, *J. Fluid Mech.* 853, 2018, pp. 333-358. <https://doi.org/10.1017/jfm.2018.566>
- [4] Bridges, J., & Brown, C. (2004). Parametric Testing of Chevrons on Single Flow Hot Jets. In 10th AIAA/CEAS Aeroacoustics Conference. 10th AIAA/CEAS Aeroacoustics Conference. American Institute of Aeronautics and Astronautics. <https://doi.org/10.2514/6.2004-2824>
- [5] Papamoschou, D. and Debiasi, M., “Directional Suppression of Noise from a High-Speed Jet,” *AIAA Journal*, Vol. 39, No. 3, 2001. <https://doi.org/10.2514/2.1345>
- [6] Zaman, K.B.M.Q., “Noise- and Flow-Field of Jets from an Eccentric Coannular Nozzle,” 42nd AIAA Aerospace Sciences Meeting and Exhibit, <https://doi.org/10.2514/6.2004-5>
- [7] Papamoschou, D., “Parametric Study of Fan Flow Deflectors for Jet Noise Suppression,” 11th AIAA/CEAS Aeroacoustics Conference, 2005. <https://doi.org/10.2514/6.2005-2890>
- [8] Zaman, K.B.M.Q. and Papamoschou, D., “Effect of a Wedge on Coannular Jet Noise,” 44th AIAA Aerospace Sciences Meeting and Exhibit, 2006. <https://doi.org/10.2514/6.2006-7>
- [9] Papamoschou, D., and Shuoe, R. S., “Effect of Nozzle Geometry on Jet Noise using Fan Flow Deflectors,” 12th AIAA/CEAS Aeroacoustics Conference (27th AIAA Aeroacoustics Conference), 2006. <https://doi.org/10.2514/6.2006-2707>
- [10] Yang, G., Allen, C., Markesteijn, A.P., Abid, H.A., Karabasov, S.A., Toropov, V., Surrogate Model-Based Acoustic Optimisation of Jet Nozzle Exit Geometry, AIAA SciTech Forum and Exposition, January 3-7, 2022, San Diego. <https://doi.org/10.2514/6.2022-0683>
- [11] Fabiano, E., Mishra, A., Yang Z., Mavriplis, D.J., Towards Adjoint-based Sensitivity Analysis for Supersonic Jet Noise, AIAA Aviation Forum, June 15-19, 2020. <https://doi.org/10.2514/6.2020-3131>
- [12] Ruscher, C., Gogineni, S., Papamoschou, D., Novel Methodology for the Rapid Acoustic Optimization of Supersonic Multi-Stream 3D Nozzles, NASA Acoustics Technical Working Group Presentation, 2021
- [13] Tam, C. K. W., Auriault, L., Jet Mixing Noise from Fine-Scale Turbulence, *AIAA Journal*, Vol. 37, No. 2, pp.145-153, 1999.
- [14] Bridges, J., Khavaran, A., and Hunter, C. A., “Assessment of Current Jet Noise Prediction Capabilities,” 14th AIAA/CEAS Aeroacoustics Conference, 5-7 May, 2008. <https://doi.org/10.2514/6.2008-2933>
- [15] Khavaran, A., Bridges, J., and Freund, B. J., “A Parametric Study of Fine-Scale Turbulence Mixing Noise,” 8th AIAA/CEAS Aeroacoustics Conference, 17-19 June 2002. <https://doi.org/10.2514/6.2002-2419>
- [16] Papamoschou, D., “New method for jet noise reduction in turbofan engines,” *AIAA journal*, Vol. 42, No. 11, 2004, pp. 2245–2253. <https://doi.org/10.2514/1.4788>
- [17] Khavaran, A., Kenzakowski, D.C., Mielke-Fagan, A.F., “Hot jets and sources of jet noise,” *International Journal of Aeroacoustics*, Vol. 9 pp. 491-532. <https://doi.org/10.1260/1475-472X.9.4-5.491>

- [18] Leib, S.J., Goldstein, M.E., “Hybrid Source Model for Predicting High-Speed Jet Noise” *AIAA Journal*, Vol. 49(7), 2011, pp.1324–1335, 2011. <https://doi.org/10.2514/1.J050707>.
- [19] Gryazev, V., Markesteijn, A.P., Karabasov, S.A. Generalised acoustic analogy modelling of hot jet noise, *AIAA Journal*, Nov, 2021. <https://doi.org/10.2514/1.J060896>
- [20] Tam, C.K., Pastouchenko, N. N., Viswanathan, K., “Fine-Scale Turbulence Noise from Hot Jets”, *AIAA Journal*. Vol. 43, No. 8 (2005), pp. 1675-1683. <https://doi.org/10.2514/1.8065>.
- [21] Lighthill, M.J., “On sound generated aerodynamically: I. General Theory.” *Proceedings of The Royal Society of London*, Vol. 211,1952, pp. 564-587. <https://doi.org/10.1098/rspa.1952.0060>.
- [22] Morris P.J., Farassat, F., “Acoustic analogy and alternative theories for jet noise prediction,” *AIAA Journal*, Vol.40(4), pp. 671-680, 2002. <https://doi.org/10.2514/2.1699>
- [23] Khavaran, A., Bridges, J., “Modelling of Turbulence Generated Noise in Jets,” 10th AIAA/CEAS Aeroacoustics Conference. 2004. <https://doi.org/10.2514/6.2004-2983>
- [24] Khavaran, A., Georgiadis, N, Bridges, J., Dippold, V., “Effect of Free Jet on Refraction and Noise,” 11th AIAA/CEAS Aeroacoustics Conference. 2005, <https://doi.org/10.2514/6.2005-2941>
- [25] Khavaran, A., Bridges, J., “An Empirical Temperature Variance Source Model in Heated Jets,” NASA Technical Memorandum, 2012
- [26] Goldstein, M.E., “A unified approach to some recent developments in jet noise theory,” *International Journal of Aeroacoustics*, Vol.1, pp. 1-16, 2002. <https://doi.org/10.1260/1475472021502640>.
- [27] Goldstein, M.E., “A generalized acoustic analogy,” *Journal of Fluid Mechanics*, Vol. 488, 2003, pp. 315-333. <https://doi.org/10.1017/S0022112003004890>.
- [28] Karabasov, S.A., Afsar, M.Z., Hynes, T.P., Dowling, A.P., McMullan, W.A., Pokora, C.D., Page, G.J., McGuirk, J.J., “Jet Noise: Acoustic Analogy informed by Large Eddy Simulation,” *AIAA Journal*., Vol. 48(7), 2010. <https://doi.org/10.2514/1.44689>.
- [29] Gryazev, V., and Karabasov, S. A., “Comparison of Two Goldstein Acoustic Analogy Implementations with the Tam&Auriault Model for Heated and Unheated Jet Noise Prediction,” *AIAA Aeroacoustics Conference*, AIAA Paper 2018-2828, June 2018. <https://doi.org/10.2514/6.2018-2828>.
- [30] Karabasov, S.A., Goloviznin, V.M., “Compact Accurately Boundary Adjusting high-REsolution Technique for Fluid Dynamics,” *Journal of Computational Physics*, Vol. 228, 2009, pp. 7426-7451. <https://doi.org/10.1016/j.jcp.2009.06.037>.
- [31] Goloviznin, V.M., Samarskii. A.A., “Finite difference approximation of convective transport equation with space splitting time derivative,” *Journal of Mathematical Modelling*, 1998, Vol. 10(1), 86–100.
- [32] Faranosov, G.A., Goloviznin, V.M., Karabasov, S.A., Kondakov, V.G., Kopiev, V.F., Zaitsev, M.A., “CABARET method on unstructured hexahedral grids for jet noise computation,” *Computers & Fluids*, Vol. 88, pp. 165-179, 2013.
- [33] Semiletov, V.A., Karabasov, S.A., “CABARET scheme with conservation-flux asynchronous timestepping for nonlinear aeroacoustics problems,” *Journal of Computational Physics*, Vol. 253, pp. 157-165, 2013. [doi:10.1016/j.jcp.2013.07.008](https://doi.org/10.1016/j.jcp.2013.07.008).

- [34] Fureby, C., Grinstein, F.F., “Large Eddy Simulation of High Reynolds Number Free and Wall Bounded Flows,” *Journal of Computational Physics*, Vol. 181, pp. 68-97, 2002. <https://doi.org/10.1006/jcph.2002.7119>.
- [35] Markesteijn, A.P., Semiletov, V.A., Karabasov, S.A., “GPU CABARET solutions for the SILOET jet noise experiment: Flow and noise modelling,” 22nd AIAA/CEAS Aeroacoustics Conference, Lyon, France 2016. <https://doi.org/10.2514/6.2016-2967>.
- [36] Markesteijn, A.P., Karabasov, S. A., “GPU-CABARET Solutions for the NASA SHJAR Jet Noise Experiment: Flow and Noise Modeling,” 23rd AIAA/CEAS Aeroacoustics Conference, 2017. <https://doi.org/10.2514/6.2017-3852>
- [37] Markesteijn, A.P., Karabasov, S.A., “CABARET solutions on graphics processing units for NASA jets: Grid sensitivity and unsteady inflow condition effect,” *Comptes Rendus Mécanique*, Vol. 346 (10), pp. 948-963, 2018. <https://doi.org/10.1016/j.crme.2018.07.004>.
- [38] Markesteijn, A.P., Karabasov, S.A., “Simulations of co-axial jet flows on graphics processing units: The flow and noise analysis,” *Philosophical Transactions of The Royal Society A*, Vol. 377, 2019. <https://doi.org/10.1098/rsta.2019.0083>.
- [39] Markesteijn, A.P., Gryazev, V., Karabasov, S.A., Ayupov, R.Sh., Benderskiy, L. A., Lyubimov, D.A. “Flow and Noise Predictions of Coaxial Jets”, *AIAA Journal*, Vol. 58(12), 2020. <https://doi.org/10.2514/1.J058881>.
- [40] Ffowcs Williams, J. E., Hawkings, D. L., “Sound generation by turbulence and surfaces in arbitrary motion,” *Philosophical Transactions of The Royal Society A*, Vol. 264, 1969, 32142. <https://doi.org/10.1098/rsta.1969.0031>.
- [41] Tam, C.K.W., Ganesan, A., “A Modified kappa - epsilon Turbulence Model for Calculating the Mean Flow and Noise of Hot Jets,” *AIAA Journal*, Vol. 42, No. 1, pp. 2634, 2004. <https://doi.org/10.2514/1.9027>.
- [42] Tam, C.K.W., Viswanathan, K., Ahuja, K. K., Panda, J. The sources of jet noise: experimental evidence, *J. Fluid Mech.*, Vol 25 November 2008, pp. 253 – 292. <https://doi.org/10.1017/S0022112008003704>
- [43] Tam, C.K.W., Auriault, L., “Mean flow refraction effects on sound from localized sources in a jet,” *Journal of Fluid Mechanics*, Vol. 370, pp. 149-174, 1998. <https://doi.org/10.1017/S0022112098001852>.
- [44] Tam, C.K.W., A phenomenological approach to jet noise: the two-source model, *Philosophical Transactions A*, 2019. <https://doi.org/10.1098/rsta.2019.0078>
- [45] Pope, S. B., *Turbulent Flows*, Cambridge University Press, 2000. <https://doi.org/10.1017/CBO9780511840531>,
- [46] Goldstein, M.E., Sescu, A., Afsar, M. Z. Effect of non-parallel mean flow on the Green’s function for predicting the low-frequency sound from turbulent air jets, *J. Fluid Mech.*, Vol. 695 , 25 March 2012 , pp. 199 – 234. <https://doi.org/10.1017/jfm.2012.12>
- [47] Harper-Bourne, M., “Jet noise turbulence measurements”, AIAA-2003-3214, 9th AIAA/CEAS Aeroacoustics Conference, 2003. <https://doi.org/10.2514/6.2003-3214>.



## Appendix A

**Table A1. Parameters of the current implementation of Tam and Auriault's, Khavaran's, and GAA models for the SILOET and SHJAR jets using the turbulent kinetic energy and dissipation rate in the definition of acoustic scales.**

| Case   | Meanflow and turbulence model | Jet  | Tam and Auriault |       |       | Khavaran |       |     |      |       |       | GAA   |       |
|--------|-------------------------------|------|------------------|-------|-------|----------|-------|-----|------|-------|-------|-------|-------|
|        |                               |      | $c_l$            | $c_r$ | $A$   | $c_l$    | $c_r$ | $a$ | $b$  | $B_c$ | $B_h$ | $c_l$ | $c_r$ |
| SILOET | RANS                          | Cold | 0.130            | 0.208 | 0.755 | 0.540    | 0.820 | 0   | 0.85 | 1     | 1     | 0.496 | 0.313 |
|        |                               | Hot  | 0.266            | 0.203 |       | 0.721    | 1.020 |     | 0.82 | 9     | 3     | 0.416 | 0.293 |
|        | LES                           | Cold | 0.220            | 0.300 |       | 0.860    | 1.570 |     | 0.8  | 4     | 1     | 0.695 | 0.550 |
|        |                               | Hot  | 0.290            | 0.230 |       | 0.820    | 0.820 |     | 0.75 | 9     | 3     | 0.586 | 0.303 |
| SHJAR  | RANS                          | SP 7 | 0.256            | 0.233 | 0.755 |          |       |     |      |       |       |       |       |
|        | LES                           | SP 7 | 0.265            | 0.220 |       |          |       |     |      |       |       |       |       |

### Definition of acoustic scales in the previous literature

|  | Tam and Auriault (1999)    |       |       | Khavaran et al. (2004) |        |     |      |   |   |
|--|----------------------------|-------|-------|------------------------|--------|-----|------|---|---|
|  | 0.256                      | 0.233 | 0.755 | 2.9430                 | 0.1846 | 0.5 | 0.25 | - | - |
|  | Morris and Farassat (2002) |       |       |                        |        |     |      |   |   |
|  | 0.130                      | 0.308 | 0.733 |                        |        |     |      |   |   |

**Table A2. Parameters of the current implementation of Tam and Auriault's, Khavaran's, and GAA models for the SILOET and SHJAR jets using the turbulent kinetic energy and meanflow vorticity in the definition of acoustic scales.**

| Case   | Meanflow and turbulence model | Jet  | Tam and Auriault |       |       | Khavaran |       |     |      |       |       | GAA   |       |
|--------|-------------------------------|------|------------------|-------|-------|----------|-------|-----|------|-------|-------|-------|-------|
|        |                               |      | $c_l$            | $c_r$ | $A$   | $c_l$    | $c_r$ | $a$ | $b$  | $B_c$ | $B_h$ | $c_l$ | $c_r$ |
| SILOET | RANS                          | Cold | 0.726            | 0.440 | 0.755 | 1.760    | 1.840 | 0   | 0.82 | 1     | 1     | 1.396 | 1.433 |
|        |                               | Hot  | 1.310            | 0.280 |       | 2.260    | 1.220 |     | 0.85 | 6     | 1     | 1.965 | 1.100 |
|        | LES                           | Cold | 1.220            | 0.550 |       | 2.960    | 3.000 |     | 0.8  | 2     | 1     | 2.190 | 1.965 |
|        |                               | Hot  | 1.650            | 0.380 |       | 2.660    | 2.800 |     | 0.8  | 9     | 2     | 1.965 | 1.100 |
| SHJAR  | RANS                          | SP 7 | 0.550            | 0.585 | 0.755 |          |       |     |      |       |       |       |       |
|        | LES                           | SP 7 | 0.950            | 0.785 |       |          |       |     |      |       |       |       |       |